Affinity profiles for human somatostatin receptor subtypes SST1–SST5 of somatostatin radiotracers selected for scintigraphic and radiotherapeutic use

Article *in* European Journal of Nuclear Medicine and Molecular Imaging · March 2000

DOI: 10.1007/s002590050034

CITATIONS
1,045

READS
1,656

7 authors, including:

Jean Claude Reubi
Universität Bern
541 PUBLICATIONS **44,765** CITATIONS

SEE PROFILE

Helmut Maecke
University Medical Center Freiburg
443 PUBLICATIONS **26,176** CITATIONS

SEE PROFILE

Affinity profiles for human somatostatin receptor subtypes SST1–SST5 of somatostatin radiotracers selected for scintigraphic and radiotherapeutic use

Jean Claude Reubi[1], Jean-Claude Schär[1], Beatrice Waser[1], Sandra Wenger[1], Axel Heppeler[2], Jörg S. Schmitt[2], Helmut R. Mäcke[2]

[1] Division of Cell Biology and Experimental Cancer Research, Institute of Pathology, University of Berne, PO Box 62, Murtenstrasse 31, CH-3010 Berne, Switzerland
[2] Department of Nuclear Medicine, Radiological Chemistry Division, University Hospital, Basel, Switzerland

Received 8 August and in revised form 26 October 1999

Abstract. In vivo somatostatin receptor scintigraphy using Octreoscan is a valuable method for the visualisation of human endocrine tumours and their metastases. Recently, several new, alternative somatostatin radioligands have been synthesised for diagnostic and radiotherapeutic use in vivo. Since human tumours are known to express various somatostatin receptor subtypes, it is mandatory to assess the receptor subtype affinity profile of such somatostatin radiotracers. Using cell lines transfected with somatostatin receptor subtypes sst1, sst2, sst3, sst4 and sst5, we have evaluated the in vitro binding characteristics of labelled (indium, yttrium, gallium) and unlabelled DOTA-[Tyr^3]-octreotide, DOTA-octreotide, DOTA-lanreotide, DOTA-vapreotide, DTPA-[Tyr^3]-octreotate and DOTA-[Tyr^3]-octreotate. Small structural modifications, chelator substitution or metal replacement were shown to considerably affect the binding affinity. A marked improvement of sst2 affinity was found for Ga-DOTA-[Tyr^3]-octreotide (IC_{50} 2.5 n*M*) compared with the Y-labelled compound and Octreoscan. An excellent binding affinity for sst2 in the same range was also found for In-DTPA-[Tyr^3]-octreotate (IC_{50} 1.3 n*M*) and for Y-DOTA-[Tyr^3]-octreotate (IC_{50} 1.6 n*M*). Remarkably, Ga-DOTA-[Tyr^3]-octreotate bound at sst2 with a considerably higher affinity (IC_{50} 0.2 n*M*). An up to 30-fold improvement in sst3 affinity was observed for unlabelled or Y-labelled DOTA-octreotide compared with their Tyr^3-containing analogue, suggesting that replacement of Tyr^3 by Phe is crucial for high sst3 affinity. Substitution in the octreotide molecule of the DTPA by DOTA improved the sst3 binding affinity 14-fold. Whereas Y-DOTA-lanreotide had only low affinity for sst3 and sst4, it had the highest affinity for sst5 among the tested compounds (IC_{50} 16 n*M*). Increased binding affinity for sst3 and sst5 was observed for DOTA-[Tyr^3]-octreotide, DOTA-lanreotide and DOTA-vapreotide when they were labelled with yttrium. These marked changes in subtype affinity profiles are due not only to the different chemical structures but also to the different charges and hydrophilicity of these compounds. Interestingly, even the coordination geometry of the radiometal complex remote from the pharmacophoric amino acids has a significant influence on affinity profiles as shown with Y-DOTA versus Ga-DOTA in either [Tyr^3]-octreotide or [Tyr^3]-octreotate. Such changes in sst affinity profiles must be identified in newly designed radiotracers used for somatostatin receptor scintigraphy in order to correctly interpret in vivo scintigraphic data. These observations may represent basic principles relevant to the development of other peptide radioligands.

Key words: Somatostatin receptor subtypes – Receptor affinity – Gallium-labelled radioligands – Yttrium-labelled radioligands – Octreotate

Eur J Nucl Med (2000) 27:273–282

Introduction

In vivo somatostatin receptor scintigraphy has been shown in the last decade to be a valuable method in humans for the visualisation of primary tumours and metastases which express somatostatin receptors, such as most neuroendocrine tumours. Although earlier studies had used radioiodinated octreotide as the radioligand [1], the gold standard for these investigations is presently indium-111 labelled DTPA-octreotide (Octreoscan) [2]. Despite good results with Octreoscan, in the last few years there have been several reports describing new, alterna-

Correspondence to: J.C. Reubi, Division of Cell Biology and Experimental Cancer Research, Institute of Pathology, University of Berne, PO Box 62, Murtenstrasse 31, CH-3010 Berne, Switzerland

tive somatostatin radioligands. Some have been synthesised with the aim of using them for the radionuclide therapy of tumours; one such example is DOTA-[Tyr^3]-octreotide, which can be labelled with yttrium-90 and was shown to be a promising agent for this type of metabolic therapy [3–5]. A further ligand which is based on another synthetic backbone molecule, lanreotide, is DOTA-lanreotide (Mauritius, see Fig. 1), which has been claimed to compare favourably with Octreoscan for diagnostic purposes [6, 7]. Vapreotide (Fig. 1) and its DTPA derivative have also recently been described as alternative radiotracers [8, 9]. Furthermore, gallium-67 labelled DOTA-[Tyr^3]-octreotide has recently been suggested to be a favourable alternative to Octreoscan [10]. Finally, molecules based on slightly modified octreotide, such as DTPA-[Tyr^3]-octreotate (Fig. 1), have been shown in animal models to be more effective for the visualisation of tumours than Octreoscan [11].

The recent cloning of several somatostatin receptor genes has increased our understanding of somatostatin receptor structure and function. To date the human somatostatin receptor subtypes sst1, sst2, sst3, sst4 and sst5 have been cloned and partially characterised [12, 13]. All five receptor subtypes can functionally couple to the inhibition of adenylate cyclase and to several other second messenger systems. Pharmacological studies have shown that all five human subtypes bind somatostatin 14 and somatostatin 28 with high affinity, whereas the sst2 subtype preferentially binds the octapeptide octreotide with very high affinity. Conversely, sst1 and sst4 do not bind octreotide whereas sst3 has an intermediate affinity and sst5 a moderately high affinity for octreotide [12, 13]. It is important to know the affinity pattern of peptide analogues foreseen to be of value for oncological applications since we know that human tumours can express several of these somatostatin receptor subtypes, each subtype with a different pattern of expression depending on the individual tumour and on the tumour type [14, 15].

It is conceivable that small structural modifications of somatostatin analogues, including the introduction of a metal in the chelator, may affect the binding properties of the analogues for the various sst subtypes. It is therefore crucial to evaluate the somatostatin receptor subtype affinity profile of new radioligands intended for the in vivo scintigraphy of tumours, in order not only to select analogues with the most adequate and unique affinity profile but also to interpret correctly the in vivo scans of the tumours performed with such ligands. Our aim was therefore to evaluate the binding affinity profile of a number of somatostatin radioligands used in nuclear medicine, by testing their affinity in cells stably transfected with the five different human somatostatin receptor subtypes. Both established and new somatostatin radioligands were included in the study. Throughout this paper, the non-radioactive metal-chelator-peptide conjugates were used as competitors to determine IC_{50} values utilising ^{125}I-[Leu^8, D-Trp^{22}, Tyr^{25}]-somatostatin 28 as radioligand. We assumed that – as generally agreed – the non-radioactive metals behave like their radioactive congeners.

Materials and methods

Peptides. The peptides studied in this investigation are listed in Table 1 and depicted in Fig. 1. Control peptides were somatostatin 28 (SS-28; Bachem, Switzerland), octreotide (Novartis, Basel, Switzerland) and the sst1-selective analogue Des-AA^{1,2,5}[Tyr^2,D-Trp^8,l-Amp^9]-somatostatin (CH288; J. Rivier, San Diego, USA; [16]). Vapreotide was a gift of Debiopharm (Lausanne). DOTA-lanreotide and DTPA-[Tyr^3]-octreotate were provided by A. Srinivasan (St. Louis, USA).

Chemical synthesis. DTPA-[Tyr^3]-octreotate was synthesised according to de Jong et al. [11]. DOTA-[Tyr^3]-octreotate was synthesised using standard Fmoc (9-fluorenylmethoxycarbonyl) strategy [17] on tritylchloride resin. The protected peptide was cleaved from the resin, cyclised, deprotected and purified by preparative high-performance liquid chromatography (HPLC) analogous to the method of Arano et al. [18]. DTPA-octreotide, DOTA-octreotide, DOTA-[Tyr^3]-octreotide, DOTA-lanreotide and DOTA-vapreotide and the In^{3+}, Ga^{3+} and Y^{3+} complexes were synthesised according to the methods described previously [19, 20]. The following non-radioactive metal isotopes were used: ^{115}In, ^{89}Y and ^{69,71}Ga. The exact mass spectra (MS) and elemental analysis of DOTA-[Tyr^3]-octreotide were as follows: electrospray-ionisation mass spectroscopy (ESI-MS): m/z=1421.7 $[M+H]^+$ (16%), 711.7 $[M+2\ H]^{2+}$ (97%), 474.7 $[M+3\ H]^{3+}$ (100%); $C_{65}H_{92}N_{14}O_{18}S_2 \cdot 7\ H_2O \cdot 0.4\ AcOH \cdot 0.05$ TFA (1577.37): calcd C 50.18 H 6.81 N 12.43; found C 50.38 H 6.74 N 12.40; amino acid analysis: Thr 0.86 (1), Cys 1.20 (2), Tyr 1.00 (1), Phe 0.99 (1), Lys 1.07 (1), Trp det. (1); purity (HPLC): >97%. The remaining peptides were characterised by ESI/MS spectra and their purity (>97% in all cases) was confirmed by reversed phase HPLC (RP-HPLC).

Determination of peptide concentrations and molar extinction coefficients. The determination of DOTA-peptide concentrations is based on knowledge of the exact elemental composition of DOTA-[Tyr^3]-octreotide. The known peptide content allowed the determination of the molar extinction coefficient ε. This was confirmed by a labelling experiment using a defined excess of $^{89}Y(NO_3)_3$ spiked with $^{90}YCl_3$ as described below. The molar extinction coefficients of the remaining DOTA/DTPA-peptides were then determined as follows: Aliquots containing approximately 50 µg of the respective peptide in 35 µl 0.01 *M* CH_3COOH were diluted with 0.1 *M* CH_3COOH to a final volume of 500 µl and the absorbance at 280 nm was recorded. Sodium acetate buffer (20 µl, 0.1 *M*, pH 5.1) and a $^{89}Y(NO_3)_3$ solution (32–36 µl, 2 m*M*) spiked with $^{90}YCl_3$ (15 MBq/500 µl) were added to a 50 µg DOTA-peptide aliquot (35 µl 0.01 *M* CH_3COOH). The reaction mixture was heated for 25 min to 95°C and incubated at room temperature for further 15 min together with DTPA (20 µl, 1 m*M*) before being injected into an HPLC system which was coupled to a gamma detector (Hewlett Packard 1050 HPLC system with a flow-through Berthold LB 506 C1 gamma detector; column: Macherey Nagel, Nucleosil 120-C_{18}; flow 0.75 ml/min; eluents: A=0.1% trifluoroacetic acid (TFA) in H_2O and B=acetonitrile (MeCN); non-linear gradient: 0–5 min, 100% A; 25 min, 75% A; 30–35 min, 100% A). The

Table 1. Peptides studied in this investigation. All cited peptides are octapeptides, cyclised by a Cys-Cys disulphide bridge. The different chelator peptide conjugates are obtained by modification of the AA (amino acid) sequence (I–V) and by conjugation to a chelator (A, DTPA or B, DOTA) (see also Fig. 1)

Peptide sequence	Name	Code
-D-Phe-Cys-Phe-D-Trp-Lys-Thr-Cys-Thr(ol)	Octreotide	I
-D-Phe-Cys-Tyr-D-Trp-Lys-Thr-Cys-Thr(ol)	[Tyr^3]-octreotide	II
-D-Phe-Cys-Tyr-D-Trp-Lys-Val-Cys-Trp-NH_2	Vapreotide	III
-β-D-NaI-Cys-Tyr-D-Trp-Lys-Val-Cys-Thr-NH_2	Lanreotide	IV
-D-Phe-Cys-Tyr-D-Trp-Lys-Thr-Cys-Thr-OH	[Tyr^3]-octreotate	V
Chelator	**Abbreviation**	**Code**
Diethylene triamine penta-acetic acid	DTPA	A
1,4,7,10-Tetraazacyclododecane-1,4,7,10-tetra-acetic acid	DOTA	B
Chelator peptide conjugate	**Abbreviation**	**Code**
DTPA-octreotide	DTPAOC	A-I
DTPA-[Tyr^3]-octreotate	DTPATATE	A-V
DOTA-octreotide	DOTAOC	B-I
DOTA-[Tyr^3]-octreotide	DOTATOC	B-II
DOTA-vapreotide	DOTAVAP	B-III
DOTA-lanreotide	DOTALAN	B-IV
DOTA-[Tyr^3]-octreotate	DOTATATE	B-V

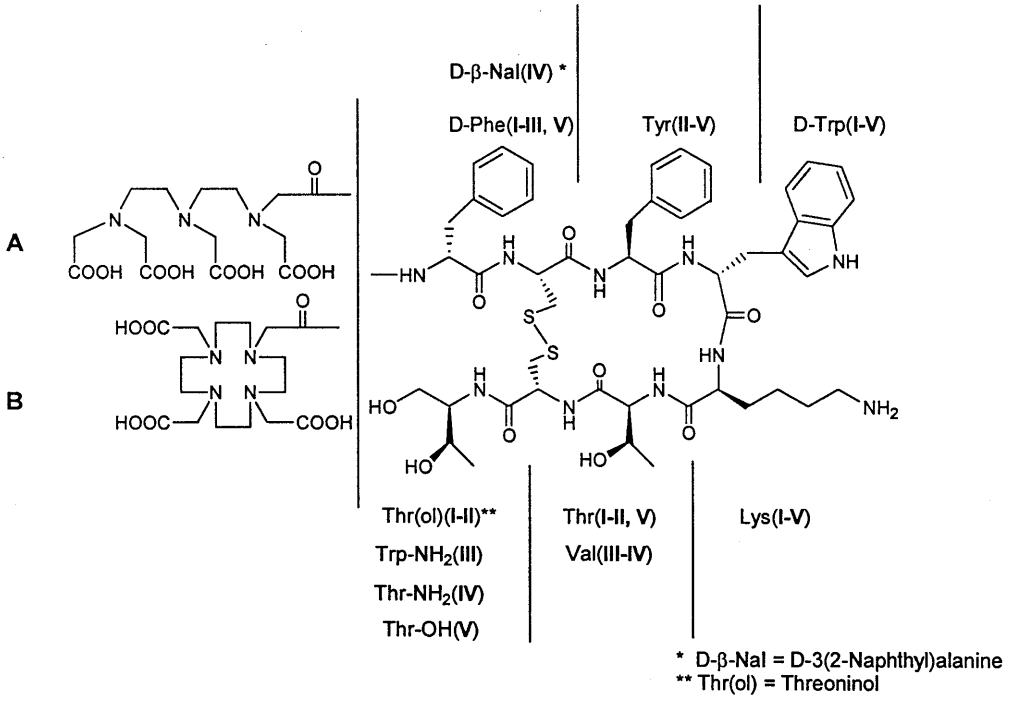

Fig. 1. Chemical structure of the parent octapeptide octreotide (I) and the different chelator peptide conjugates DTPA-octreotide (**A**-I), DTPA-[Tyr^3]-octreotate (**A**-V), DOTA-octreotide (**B**-I), DOTA-[Tyr^3]-octreotide (**B**-II), DOTA-vapreotide (**B**-III), DOTA-lanreotide (**B**-IV), and DOTA-[Tyr^3]-octreotate (**B**-V) obtained by modification of the AA (amino acid) sequence (I–V) and by conjugation to a chelator (**A**, DTPA or **B**, DOTA)

concentration, determined by calculating the ratio of the $^{89/90}$Y-DTPA/$^{89/90}$Y-DOTA-peptide peaks, was compared with the value obtained from elemental analysis. By knowing the exact concentration and the absorbance at 280 nm of the aliquot it was possible to calculate the molar extinction coefficient of the respective DOTA-peptide conjugate (Table 2). These values were compared (a) with literature values [21] by adding up the molar extinction coefficients ε_{280} of the amino acids which make a significant contribution to the absorption at λ=280 nm (Trp, βNaI, Tyr, Cys_2); (b) with values observed by measuring a mixture of all amino acids plus chelator (see Table 2). The ε_{280} values of the respective DTPA conjugates were shown to be the same as those of the DOTA conjugates. For the calculation of concentration the experimentally determined ε_{280} values were used.

Cell culture. CHO-K1 cells stably expressing human sst1 and sst5 were kindly provided by Drs. T. Reisine and G. Singh (University of Pennsylvania, Philadelphia, Pa.) and CCL39 cells stably expressing human sst2, sst3 and sst4 by Dr. D. Hoyer (Novartis Pharma, Basel, Switzerland). CHO-K1 cells were grown in Ham's F-12 medium and CCL39 cells in Dulbecco's modified Eagle's medium/Ham's F-12 (1:1) mix, supplemented with 10% foetal bo-

Table 2. Comparison of the molar extinction coefficients: experimentally observed ε_{max} (obs), and calculated ε_{max} derived (a) by adding together the molar extinction coefficients ε_{280} of the amino acids which make a significant contribution to the absorption at λ=280 nm, or (b) by measuring a mixture of all amino acids plus chelator ε_{280}

Peptide	ε_{280} (obs)	ε_{280} (a)	ε_{280} (b)
DOTA-octreotide	6575	5700	5867
DOTA-[Tyr^3]-octreotide	6849	7040	6811
DOTA-lanreotide	11,129	–	10,977
DOTA-vapreotide	13,500	12,590	12,139

The ε_{280} values of the respective DTPA conjugates were shown to be the same as those of the DOTA conjugates

vine serum, 100 U/ml penicillin and 100 µg/ml streptomycin, in humidified air containing 5% CO_2 at 37°C. Geneticin (G418-sulfate; Gibco, USA) was used where necessary to maintain selection pressure at a final concentration of 400 µg/ml for sst2- to sst4- and 285 µg/ml for sst5-expressing cells as described previously [22–24]. All culture reagents were supplied by Gibco BRL, Life Technologies (Grand Island, N.Y.).

In situ hybridisation histochemistry. To control adequacy of the cell material, in situ hybridisation for human sst mRNAs was performed on CHO-K1 and CCL39 cells expressing the different sst receptor subtypes. Cells were detached from culture flasks by washing with Puck's Saline A and brief incubation with trypsin (0.5 mg/ml)/EDTA (0.2 mg/ml), collected by centrifugation, and resuspended in phosphate-buffered saline at a final cell density of approximately 6×10^4 cells/µl; 25-µl aliquots of cell suspension were spotted onto microscopic slides, air dried and stored at –20°C. They were subsequently fixed with 4% formaldehyde, washed with phosphate-buffered saline, air dried and stored at 4°C under dry conditions. Cell smears were then used for sst1, sst2, sst3, sst4 and sst5 mRNA detection by in situ hybridisation. The protocol followed was essentially that described in detail previously [14].

Oligonucleotide probes complementary to the sst1, sst2, sst3 [14], sst4 and sst5 [25] mRNAs were synthesised and purified on a 20% polyacrylamide-8 *M* urea sequencing gel (Microsynth, Balgach, Switzerland). They were labelled at the 3'-end by using [α-^{32}P]dATP (>3000 Ci/mmol; NEN Life Science Products, Boston, Mass.) and terminal deoxynucleotidyltransferase (Boehringer, Mannheim, Germany) to specific activities of 33.3–74 GBq/mmol. Control experiments were carried out with the probes used in the present study to determine the specificity of the hybridisation signal obtained, as described previously [14].

These control in situ hybridisation studies confirmed that the five cell lines used for the study expressed the correct sst mRNA.

Receptor autoradiography. Cells were washed twice with and scraped into ice-cold 0.05 *M* Tris-HCl (pH 7.4), collected by centrifugation, and homogenised using a rotor/stator slash system (Polytron, Kinematica Inc., Littau, Switzerland) in the same buffer. After centrifugation at 120 *g* for 5 min at 4°C, the supernatant was collected and centrifuged again at 48,000 *g* for 30 min at 4°C. The resulting pellet was resuspended in ice-cold Tris buffer, transferred into a microfuge tube, and centrifuged at 20,000 *g* for 15 min at 4°C. After withdrawal of the supernatant, the membrane pellet was stored at –80°C.

Receptor autoradiography was performed on 20-µm-thick cryostat (Leitz 1720, Rockleigh, N.J.) sections of the membrane pellets, mounted on microscope slides and then stored at –20°C. For each of the tested compounds, complete displacement experiments were performed with the universal somatostatin radioligand ^{125}I-[Leu^8, D-Trp^{22}, Tyr^{25}]-somatostatin 28 using increasing con-

Table 3. Affinity profiles (IC_{50}) for human sst1–sst5 receptors of a series of somatostatin analogues

Peptides	hsst 1	hsst 2	hsst 3	hsst 4	hsst 5
SS-28	5.2±0.3 (19)	2.7±0.3 (19)	7.7±0.9 (15)	5.6±0.4 (19)	4.0±0.3 (19)
Octreotide	>10,000 (5)	2.0±0.7 (5)	187±55 (3)	>1,000 (4)	22±6 (5)
CH288	23±2 (3)	>10,000 (4)	>1,000 (3)	>10,000 (3)	>1,000 (4)
DTPA-octreotide	>10,000 (6)	12±2 (5)	376±84 (5)	>1,000 (5)	299±50 (6)
In-DTPA-octreotide	>10,000 (5)	22±3.6 (5)	182±13 (5)	>1,000 (5)	237±52 (5)
DOTA-TOC	>10,000 (7)	14±2.6 (6)	880±324 (4)	>1,000 (6)	393±84 (6)
Y-DOTA-TOC	>10,000 (4)	11±1.7 (6)	389±135 (5)	>10,000 (5)	114±29(5)
DOTA-LAN	>10,000 (7)	26±3.4 (6)	771±229 (6)	>10,000 (4)	73±12 (6)
Y-DOTA-LAN	>10,000 (3)	23±5 (4)	290±105 (4)	>10,000 (4)	16±3.4 (4)
DOTA-VAP	>10,000 (3)	29±7 (4)	419±104 (4)	743±190 (3)	80±19 (4)
Y-DOTA-VAP	>10,000 (4)	12±2 (5)	102±25 (5)	778±225 (5)	20±2.3 (5)
DOTA-OC	>10,000 (3)	14±3 (4)	27±9 (4)	>1,000 (4)	103±39 (3)
Y-DOTA-OC	>10,000 (5)	20±2 (5)	27±8 (5)	>10,000 (4)	57±22 (4)
Ga-DOTA-TOC	>10,000 (6)	2.5±0.5 (7)	613 ±140 (7)	>1,000 (6)	73±21 (6)
Ga-DOTA-OC	>10,000 (3)	7.3±1.9 (4)	120±45 (4)	>1,000 (3)	60±14 (4)
DTPA-[Tyr^3]-octreotate	>10,000 (4)	3.9±1 (4)	>10,000 (4)	>1,000 (4)	>1,000 (4)
In-DTPA-[Tyr^3]-octreotate	>10,000 (3)	1.3±0.2 (3)	>10,000 (3)	433±16 (3)	>1,000 (3)
DOTA-[Tyr^3]-octreotate	>10,000 (3)	1.5±0.4 (3)	>1,000 (3)	453±176 (3)	547±160 (3)
Y-DOTA-[Tyr^3]-octreotate	>10,000 (3)	1.6±0.4 (3)	>1,000 (3)	523±239 (3)	187±50 (3)
Ga-DOTA-[Tyr^3]-octreotate	>10,000 (3)	0.2±0.04 (3)	>1,000 (3)	300±140 (3)	377±18 (3)

All values are IC_{50}±SEM in n*M*. The number of experiments is in parentheses

centrations of the unlabelled peptide ranging from 0.1 to 1000 n*M*. The unlabelled, universal somatostatin 28 was run in parallel using the same increasing concentrations, as control. IC_{50} values were calculated after quantification of the data using a computer-assisted image processing system as described previously [26]. Tissue standards (autoradiographic [^{125}I] microscales, Amersham) containing known amounts of isotope, cross-calibrated to tissue-equivalent ligand concentrations, were used for quantification [27]. Compared with binding on cell homogenates, the present method using receptor autoradiography with sectioned cell pellets has the advantage (in addition to an economy on cells and greater flexibility) of greater inter-assay reliability and reproducibility, since the same embedded pellet can be used for successive experiments. As a minor disadvantage, IC_{50} values are somewhat higher than in the homogenate binding assay.

In addition, a Scatchard analysis was performed using ^{67}Ga-DOTA-[Tyr^3]-octreotide saturated with non-radioactive Ga^{3+} using a homogenate of rat brain cortex membranes as described previously [28].

Results

Table 3 shows the various somatostatin analogues investigated and their respective IC_{50} for the five somatostatin receptor subtypes. We used as unlabelled control peptide the natural somatostatin 28, which binds with high affinity to all five sst; as further controls, we used the sst2-selective octreotide and the sst1-selective CH288 [16]. Unlabelled and In-labelled DTPA-octreotide (Octreoscan) was furthermore used as control, the latter representing the gold standard used routinely for in vivo scintigraphy. The other investigated peptides were: unlabelled and Y-labelled DOTA-[Tyr^3]-octreotide; unlabelled and Y-labelled DOTA-lanreotide; unlabelled and Y-labelled DOTA-octreotide; unlabelled and Y-labelled DOTA-vapreotide; Ga-labelled DOTA-[Tyr^3]-octreotide and Ga-labelled DOTA-octreotide; unlabelled and In-labelled DTPA-[Tyr^3]-octreotate; and unlabelled, Y- or Ga-labelled DOTA-[Tyr^3]-octreotate. The rank order of affinity for all control substances used in the present study was compatible with the values reported in the literature, indicating that the used methodology and cells were adequate. In addition, a Scatchard analysis of one of the potent sst2-selective analogues, ^{67}Ga-DOTA-[Tyr^3]-octreotide, was performed using rat brain cortex membranes and allowed comparison with the presented IC_{50} values.

The universal ligand somatostatin 28 and the sst1-selective analogue CH288 displayed high binding affinity to the sst1 receptor whereas all the other compounds tested showed no binding.

The universal ligand somatostatin 28 but also octreotide, lanreotide, vapreotide analogues and the [Tyr^3]-octreotate analogues displayed high binding affinity for the sst2 receptors. Interestingly, however, small structural changes resulted in significant differences in binding affinity profiles. One important change was the marked improvement of sst2 affinity for Ga-labelled DOTA-[Tyr^3]-octreotide compared with Y-labelled DOTA-[Tyr^3]-octreotide, which itself was better than Octreoscan. Furthermore, unlabelled or In-labelled DTPA-[Tyr^3]-octreotate as well as unlabelled and Y-labelled DOTA-[Tyr^3]-octreotate showed better sst2 binding affinity than unlabelled or In-labelled DTPA-octreotide and unlabelled or Y-labelled DOTA-[Tyr^3]-octreotide (Table 3). Remarkably, when gallium was attached to the DOTA-[Tyr^3]-octreotate molecule, an eightfold improvement in binding affinity was observed (Table 3). No binding affinity was found for the sst1-selective analogue CH288. Figure 2 shows a typical example of the particularly high affinity of sst2 receptors for Ga-labelled DOTA-[Tyr^3]-octreotate, Ga-labelled DOTA-[Tyr^3]-octreotide and In-labelled DTPA-octreotate compared with Y-labelled DOTA-[Tyr^3]-octreotide, the con-

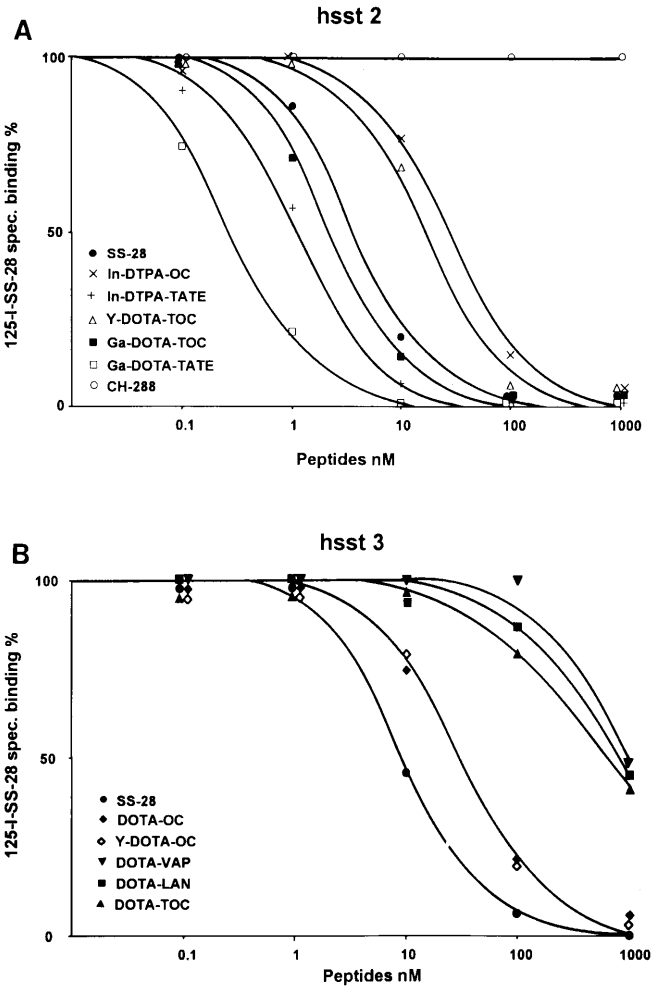

Fig. 2A, B. Competition experiments using ^{125}I-[Leu^8, D-Trp^{22}, Tyr^{25}]-somatostatin 28 as radioligand with increasing concentrations of various somatostatin analogues. **A** sst2-expressing cells; **B** sst3-expressing cells. *TOC*, [Tyr^3]-octreotide; *OC*, octreotide; *TATE*, [Tyr^3]-octreotate; *VAP*, vapreotide; *LAN*, lanreotide. Highest sst2 binding affinity is shown by Ga-DOTA-TATE. Highest sst3 binding affinity is shown by DOTA-OC and Y-DOTA-OC

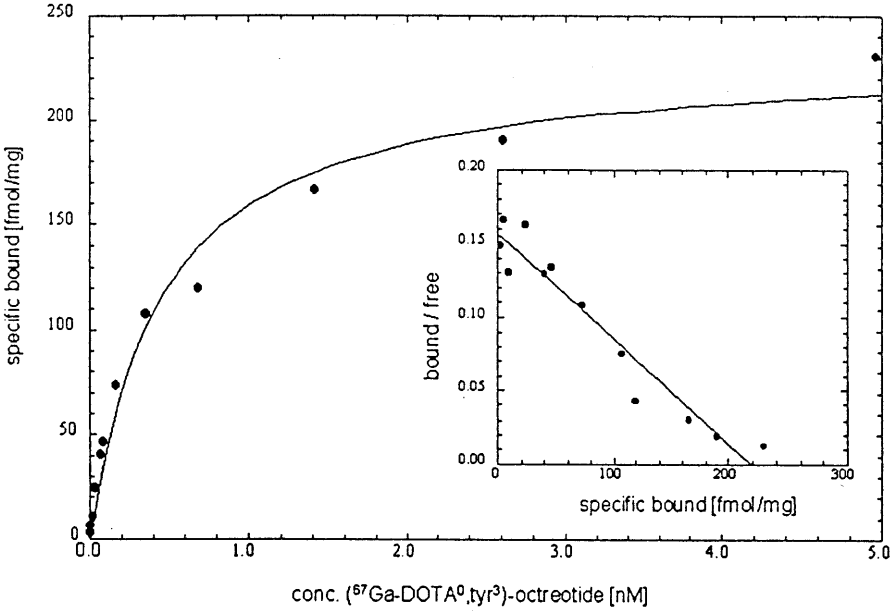

Fig. 3. Saturation binding curve of ^{67}Ga-DOTA-[Tyr^3]-octreotide using rat brain cortex membranes (*inset*: Scatchard plot analysis). K_D was calculated to be 0.45±0.11 n*M* from a fit to the saturation curve

trol molecule In-labelled DTPA-octreotide and the inactive CH288. Moreover, a Scatchard analysis of ^{67}Ga-DOTA-[Tyr^3]-octreotide binding with rat brain cortex membranes gave a K_D value of 0.45±0.11 n*M* for this compound (Fig. 3), indicative of high affinity and comparing well with the presented IC_{50} values.

Interestingly, except for the universal binder somatostatin 28, DOTA-octreotide and Y-DOTA-octreotide showed the highest binding affinity for the sst3 receptor. Those two compounds were 7 times more potent than In-DTPA-octreotide and up to 30 times more potent than the [Tyr^3]-containing DOTA-[Tyr^3]-octreotide or DOTA-lanreotide analogues. Y-labelling of DOTA-[Tyr^3]-octreotide, DOTA-lanreotide or DOTA-vapreotide increased the binding affinity for the sst3 significantly compared with the non-labelled molecules. Moreover, substitution in the octreotide molecule of DTPA by DOTA improved 14-fold the sst3 binding affinity. Figure 2 shows the particularly high affinity of sst3 receptors for DOTA-octreotide and Y-DOTA-octreotide compared with DOTA-[Tyr^3]-octreotide and DOTA-lanreotide. Important information provided by these studies is that replacement of Tyr^3 by the more lipophilic Phe results in considerable improvements in sst3 binding affinity.

The universal ligand somatostatin 28 bound with high affinity to the sst4 receptors, as expected. Neither DOTA-lanreotide nor Y-DOTA-lanreotide showed significant high binding affinity (Table 3). None of the other compounds tested showed a high binding affinity to sst4, the least inactive compounds being the octreotate (the most hydrophilic in the series) and vapreotide (the most lipophilic) derivatives. Figure 4 compares the affinities of Y-DOTA-vapreotide with those of Y-DOTA-octreotide, Y-DOTA-[Tyr^3]-octreotide and Y-DOTA-lanreotide.

The universal ligand SS28 as well as octreotide bound with high affinity to the sst5 receptors. Interestingly enough, the chelator-linked compounds having the highest affinity for sst5 were Y-DOTA-lanreotide and Y-DOTA-vapreotide and, to a lesser extent, Ga-DOTA-[Tyr^3]-octreotide and Ga-DOTA-octreotide. Of further interest is the fact that the Y-labelling of DOTA-[Tyr^3]-octreotide, DOTA-lanreotide or DOTA-vapreotide increased their binding affinity for the sst5 subtype significantly compared with the unlabelled molecules, as found for the sst3 receptor. Figure 4 shows that Y-labelled DOTA-lanreotide has a high affinity and Y-labelled DOTA-[Tyr^3]-octreotide a much lower affinity for sst5 receptors. As shown in Table 3, the affinities for unlabelled DOTA-[Tyr^3]-octreotide and DOTA-lanreotide were even lower than for the Y-labelled corresponding molecules.

In this series the best sst2 compound was by far Ga-labelled DOTA-[Tyr^3]-octreotate, followed by In-labelled DTPA-[Tyr^3]-octreotate, Y-labelled and unlabelled DOTA-[Tyr^3]-octreotate, and Ga-labelled DOTA-[Tyr^3]-octreotide. The best sst3 compound was the unlabelled or Y-labelled DOTA-octreotide and the best sst5 compounds were Y-labelled DOTA-lanreotide and DOTA-vapreotide. Y-labelled DOTA-lanreotide had a comparable affinity for sst2 and sst5 receptors, whereas it had a much lower affinity for sst3 and no affinity for sst1 or sst4. Except for its good sst5 affinity, the affinity profile of this compound for other sst was not better than that of In-DTPA-octreotide.

Discussion

This is the first study reporting on sst subtyping of a number of metallopeptides using metals having radioisotopes of interest in nuclear medicine (metal-chelator-peptide conjugates). The main message is that small

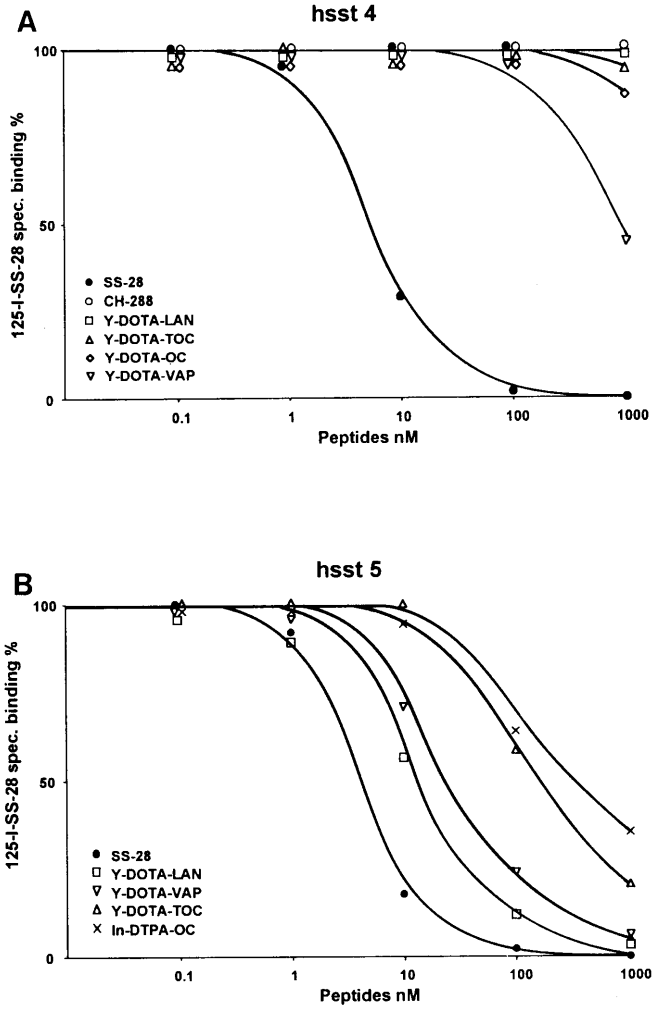

Fig. 4A, B. Competition experiments using ^{125}I-[Leu^{8}, D-Trp^{22}, Tyr^{25}]-somatostatin 28 as radioligand with increasing concentrations of various somatostatin analogues. **A** sst4-expressing cells; **B** sst5-expressing cells. *TOC*, [Tyr^{3}]-octreotide; *OC*, octreotide; *VAP*, vapreotide; *LAN*, lanreotide. Highest sst5 binding affinity is shown by Y-DOTA-LAN, which is inactive at sst4

structural changes in the radioligand molecule, the introduction of a metal, the replacement of one metal by another or the replacement of one chelator by another may provoke considerable alterations in the binding affinity for selected sst subtypes and may have an important impact on the quality of in vivo scintigraphy. Structural changes of ligands may in some cases improve the binding affinity for a particular subtype while diminishing the affinity for another sst subtype.

Significant findings include a fivefold improvement in sst2 binding affinity with labelled DOTA-[Tyr^{3}]-octreotide when yttrium was replaced by gallium. This gallium-labelled tracer showed 9 times more affinity than Octreoscan. Furthermore, In-DTPA-[Tyr^{3}]-octreotate and Y-DOTA-[Tyr^{3}]-octreotate respectively showed 17 and 14 times better binding affinity for sst2 than does Octreoscan. Most remarkable, however, is the finding that addition of gallium to DOTA-[Tyr^{3}]-octreotate brought about an eightfold improvement in affinity compared with Y-DOTA-[Tyr^{3}]-octreotate. A more than tenfold improvement in sst3 binding affinity was observed for DOTA-octreotide or Y-DOTA-octreotide compared with their [Tyr^{3}]-containing analogues. A similar improvement in sst3 affinity was also seen for Ga-DOTA-octreotide compared with its [Tyr^{3}]-containing analogue, suggesting that replacement of Tyr^{3} by Phe is particularly useful in providing high sst3 affinity. Moreover, substitution of a chelator, DTPA, by DOTA in the octreotide molecule improved 14-fold its sst3 binding affinity. Furthermore, the addition of yttrium to DOTA-[Tyr^{3}]-octreotide, DOTA-lanreotide or DOTA-vapreotide produced a two- to fivefold increase in binding affinity for sst3 and/or sst5 compared with the respective unlabelled analogues. Y-DOTA-lanreotide showed 15 times more affinity for sst5 than Octreoscan; however, it did not differ considerably from Octreoscan in its affinity for the other sst subtypes, in contrast to a recent report by Virgolini and co-workers suggesting that Y- and In-DOTA-lanreotide are universal binders to somatostatin receptors, with high affinity for sst2, sst3, sst4 and sst5 and moderate to low affinity for sst1 [6, 7]. Yttrium-labelled DOTA-vapreotide was found to show better binding affinity than Y-labelled DOTA-lanreotide, in particular with respect to sst subtypes 2 and 3, and even 4.

How can these observed changes in affinity be explained in relation to the structural modifications? The five DOTA-peptides and their Y-labelled derivatives differ with regard to their hydrophilicity. The hydrophilicity order as determined by RP-HPLC is DOTA-[Tyr^{3}]-octreotate >DOTA-[Tyr^{3}]-octreotide >DOTA-octreotide >DOTA-lanreotide >DOTA-vapreotide (data not shown). It appears that the lower hydrophilicity helps to improve the affinity for subtypes 3–5, with DOTA-vapreotide being the best binder to sst2–5. Binding affinity for hsst5 (h=human) and to a lesser extent hsst3 is clearly improved upon complexation of the DOTA-peptides with a metal, with an approximately fourfold increase. Overall charge also influences the binding pattern; whereas DTPA-octreotide and In-DTPA-octreotide still showed some affinity to hsst3 and hsst5 in the sub μ*M* range, the corresponding octreotate ligands carrying one more negative charge [Thr instead of Thr(ol)] lost this affinity. A difference in charge of the molecule with respect to the metal-free conjugate is introduced with the addition of yttrium and gallium. Remarkable and unexpected is also the improvement in sst3 binding affinity after replacement of the Tyr^{3} in the Y-DOTA-[Tyr^{3}]-octreotide molecule by Phe. The more hydrophilic Tyr allows the formation of hydrogen bonds, and this apparently results in a decreased affinity for sst2 but a higher affinity to sst3 and sst5. Little difference was found between complexed and uncomplexed DOTA-peptide binding affinity for sst2, except for the outstanding binding affinity of Ga-DOTA-[Tyr^{3}]-octreotate and Ga-DOTA-[Tyr^{3}]-

octreotide. We assume that the metal coordination geometry differences are responsible for this. As shown by X-ray crystal structures, in the model peptide complex Ga-DOTA-D-PheNH$_2$ the metal is coordinated in a pseudo-octahedral way with one uncomplexed carboxylate group as well as a free amide group, which introduces high flexibility. In Y-DOTA-D-PheNH$_2$ the coordination number is 8 including the amide oxygen; all potential chelating groups are used to encapsulate the yttrium. This metal complex is more rigid and compact and lacks the flexibility of the Ga-labelled compound. The open and flexible structure of the Ga complex may allow the octapeptide to adjust more easily to the ideal conformation for receptor binding whereas the coordinative use of the amide oxygen forces the chelate closer to the peptide, introducing some steric strain [19].

These in vitro data may explain many of the recently reported in vivo scintigraphic data obtained in animals and humans. For instance, in a preliminary comparative study with Octreoscan, ^{67}Ga-DOTA-[Tyr^3]-octreotide has been shown to provide better visualisation of human tumours [10]. This may be due to the improvement in affinity for sst2 and sst5, as it is well known that a majority of human tumours express predominantly sst2 and to a lesser extent sst5. In- and Y-labelled DOTA-lanreotide have been reported by some authors to be excellent radiotracers for many human tumours, possibly owing to their high affinity for almost all sst subtypes except sst1 [6, 7]. However, our in vitro binding data do not support the conclusions of these previous in vitro investigations completely, since we did not find a high binding affinity of Y-labelled DOTA-lanreotide for sst3 and sst4 subtypes. The reported improvement in in vivo visualisation using In-DOTA-lanreotide as compared with Octreoscan in some cases may therefore be due primarily to the higher affinity of this compound for sst5. Interestingly, the human tumours identified with ^{111}In-DOTA-lanreotide have included colorectal carcinomas [7], which have been shown to express an abundance of sst5 mRNA [29, 30], whereas sst2 mRNA was rather low. Our in vitro binding data would predict that ^{90}Y-labelled DOTA-lanreotide may not be preferable as a radiotherapeutic agent to any of the other ^{90}Y-labelled peptide conjugates, and that ^{111}In-DOTA-lanreotide, which has been evaluated for gamma scintigraphy [7], may not be preferable as a radiotracer to Octreoscan, except for tumours expressing sst5 receptors. In animal models, it has recently been reported that octreotate analogues are better able than Octreoscan to better visualise animal tumours [11]. This observation may be due to the increased affinity of octreotate analogues for sst2 receptors; this would fit with the observation that the animal tumour model used in the mentioned study primarily expresses sst2.

Although the in vivo metabolism, excretion pathway and retention times of a molecule are important parameters for its evaluation as a new radiotracer for diagnosis or therapy, there is no doubt that the in vitro characterisation of the receptor binding affinity of such a molecule is crucial information which should be obtained at an early stage of development. If several receptor subtypes exist for a particular receptor, as is the case for the somatostatin receptor, the receptor affinity investigations should be extended to all receptor subtypes. As is apparent from the present study, each radiotracer has its own typical sst receptor subtype affinity pattern; testing such compounds in vivo in animal tumour models and comparing them with other radiotracers implies that one also has to know the pattern of expression of the receptor subtypes present in the respective animal tumours. Without such knowledge it would be extremely difficult to interpret the acquired scintigraphic binding and biodistribution data. The same difficulty in interpreting qualitative and quantitative differences among various radiotracers must be considered when performing in vivo scans in tumour patients; indeed, each human tumour is known to express a pattern of sst receptor subtypes unique to that individual tumour [14, 15].

A number of clinically relevant considerations may be raised on the basis of the present results.

1. Since most somatostatin receptor-positive human tumours express the sst2 receptor subtype, an improvement in the affinity for the sst2 receptor, as seen in particular with Ga-labelled DOTA-[Tyr^3]-octreotate but also with Ga-labelled DOTA-[Tyr^3]-octreotide or In-labelled DTPA-[Tyr^3]-octreotate, may represent a considerable advantage reflected by better tumour visualisation. Since preliminary in vivo data seem to confirm such an advantage over Octreoscan, further clinical development of compounds with improved sst2 affinity should be undertaken.

2. In- and Y-DOTA-lanreotide have been claimed to be outstanding radiotracers binding with high affinity to all but one sst receptor subtype [6, 7], but our study did not identify a high binding affinity of the Y-complexed form for sst3 and sst4, suggesting that the compound may not be adequate for identification of sst3 and sst4 subtypes. However, considering its relatively high affinity for sst5 and given that several human tumours, such as pituitary adenomas [15, 31] and colorectal cancers [29, 30], are known to express sst5, this compound may, under certain conditions, be better than Octreoscan for the visualisation of these tumours. Nevertheless, it appears that radiolabelled DOTA-lanreotide is by no means a universal somatostatin radiotracer; Y-labelled DOTA-vapreotide and Ga-labelled DOTA-octreotide seem to be more appropriate in this respect, although still far from optimal candidates.

3. The role of sst3 receptors in human tumours has not yet been fully established [32, 33], nor has the incidence of sst3 expression in human tumours been documented in detail [14, 15]. Although Virgolini et al. [34] have shown an unexpectedly high expression of sst3 in several tumours, in particular exocrine pancreatic cancers, such high expression could not be found by others

[29]. New radiotracers with high affinity for sst3, such as DOTA-octreotide, may both improve our understanding of the role of this receptor subtype in humans, and permit evaluation of the incidence of its expression.

Acknowledgements. We acknowledge the gift of octreotide (Sandoz Pharma, Basel), vapreotide (Debiopharm, Lausanne), CH288 (J. Rivier, San Diego, USA) and DOTA-lanreotide and DTPA-[Tyr^3]-octreotate (synthesised by A. Srinivasan at Mallinckrodt Inc., St. Louis, USA). This work was supported in part by the Swiss National Science Foundation grant No. 31-52969.97 (to A.H. and H.R.M.). We acknowledge the expert technical assistance of P. Powell.

References

1. Krenning EP, Bakker WH, Breeman WAP, Koper JW, Kooij PPM, Ausema L, Lameris JS, Reubi JC, Lamberts SWJ. Localisation of endocrine-related tumours with radioiodinated analogue of somatostatin. *Lancet* 1989; I:242–244.
2. Krenning EP, Kwekkeboom DJ, Pauwels S, Kvols LK, Reubi JC. *Somatostatin receptor scintigraphy*. New York: Raven Press, 1995.
3. de Jong M, Bakker WH, Krenning EP, Breeman WAP, van der Pluijm ME, Bernard BF, Visser TJ, Jermann E, Béhé M, Powell P, Mäcke HR. Yttrium-90 and indium-111 labelling, receptor binding and biodistribution of [DOTA^0,D-Phe^1, Tyr^3]octreotide, a promising somatostatin analogue for radionuclide therapy. *Eur J Nucl Med* 1997; 24:368–371.
4. Otte A, Jermann E, Behe M, Goetze M, Bucher HC, Roser HW, Heppeler A, Mueller-Brand J, Maecke HR. DOTATOC: a powerful new tool for receptor-mediated radionuclide therapy. *Eur J Nucl Med* 1997; 24:792–795.
5. Otte A, Mueller-Brand J, Dellas S, Nitzsche EU, Herrmann R, Maecke HR. Yttrium-90-labelled somatostatin-analogue for cancer treatment. *Lancet* 1998; 351:417–418.
6. Smith-Jones P, Bischof C, Leimer D, Gludovacz D, Angelberger P, Pangerl T, Peck-Radosavljevic M, Hamilton G, Kaserer K, Steiner G, Schlagbauer-Wadl H, Mäcke H, Virgolini I. "Mauritius", a novel somatostatin analog for tumor diagnosis and therapy. *J Nucl Med* 1998; 39 Suppl:223P.
7. Virgolini I, Szilvasi I, Kurtaran A, Angelberger P, Raderer M, Havlik E, Vorbeck F, Bischof C, Leimer M, Dorner G, Kletter K, Niederle B, Scheithauer W, Smith-Jones P. Indium-111-DOTA-lanreotide: biodistribution, safety and radiation absorbed dose in tumor patients. *J Nucl Med* 1998; 39:1928–1936.
8. Breeman WAP, van Hagen PM, Kwekkeboom DJ, Visser TJ, Krenning EP. Somatostatin receptor scintigraphy using [^{111}In-DTPA^0]RC-160 in humans: a comparison with [^{111}In-DTPA^0]octreotide. *Eur J Nucl Med* 1998; 25:182–186.
9. Zamora PO, Guhlke S, Bender H, Diekmann D, Rhodes BA, Biersack H, Knapp FF Jr. Experimental radiotherapy of receptor-positive human prostate adenocarcinoma with ^{188}Re-RC-160, a directly-radiolabelled somatostatin analogue. *Int J Cancer* 1996; 65:214–220.
10. Heppeler A, Béhé M, Froidevaux S, Hennig M, Jermann E, Maecke HR. Metal coordination chemical aspects and tumor targeting of a promising somatostatin analogue. *J Nucl Med* 1998; 39 Suppl:63P.
11. de Jong M, Breeman WAP, Bakker WH, Kooij PPM, Bernard BF, Hofland LJ, Visser TJ, Srinivasan A, Schmidt MA, Erion JL, Bugaj JE, Mäcke HR, Krenning EP. Comparison of ^{111}In-labelled somatostatin analogues for tumor scintigraphy and radionuclide therapy. *Cancer Res* 1998; 58:437–441.
12. Hoyer D, Bell GI, Berelowitz M, Epelbaum J, Feniuk W, Humphrey PPA, O'Carroll A, Patel YC, Schönbrunn A, Taylor JE, Reisine T. Classification and nomenclature of somatostatin receptors. *Trends Pharmacol Sci* 1995; 16:86–88.
13. Reisine T, Bell GI. Molecular biology of somatostatin receptors. *Endocr Rev* 1995; 16:427–442.
14. Reubi JC, Schaer JC, Waser B, Mengod G. Expression and localization of somatostatin receptor SSTR1, SSTR2 and SSTR3 mRNAs in primary human tumors using in situ hybridization. *Cancer Res* 1994; 54:3455–3459.
15. Schaer JC, Waser B, Mengod G, Reubi JC. Somatostatin receptor subtypes sst1, sst2, sst3, and sst5 expression in human pituitary, gastroenteropancreatic and mammary tumors: comparison of mRNA analysis with receptor autoradiography. *Int J Cancer* 1997; 70:530–537.
16. Reubi JC, Schaer JC, Waser B, Hoeger C, Rivier J. A selective analog for the somatostatin receptor subtype sst1 expressed by human tumors. *Eur J Pharmacol* 1998; 345:103–110.
17. Atherton E, Sheppard RC. *Fluorenylmethoxycarbonyl-polyamide solid phase peptide synthesis. General principles and development*. Oxford: Information Press, 1989.
18. Arano Y, Akizawa H, Uezono T, Akaji K, Ono M, Funakoshi S, Koizumi M, Yokoyama A, Kiso Y, Saji H. Conventional and high-yield synthesis of DTPA-conjugated peptides: application of a monoreactive DTPA to DTPA-D-Phe^1-octreotide synthesis. *Bioconjug Chem* 1997; 8:442–446.
19. Heppeler A, Froidevaux S, Mäcke HR, Jermann E, Béhé M, Powell P, Hennig M. Radiometal-labelled macrocyclic chelator-derivatised somatostatin analogue with superb tumour-targeting properties and potential for receptor-mediated internal radiotherapy. *Chem Eur J* 1999; 5:1974–1981.
20. Béhé M, Heppeler A, Mäcke HR. New somatostatin analogs for SPECT and PET. *Eur J Nucl Med* 1996; :1144 No. OWe450.
21. Wetlaufer DB. Ultraviolet spectra of proteins and amino acids. In: Anfinsen CB Jr, Anson ML, Bailey K, Edsall JT, eds. *Advances in protein chemistry*. New York: Academic Press; 1962:303–378.
22. Rens-Domiano S, Reisine T. Biochemical and functional properties of somatostatin receptors. *J Neurochem* 1992; 58:1987–1996.
23. OCaroll A, Raynor K, Lolait SJ, Reisine T. Characterization of cloned human somatostatin receptor SSTR5. *Mol Pharmacol* 1994; 46:291–298.
24. Siehler S, Seuwen K, Hoyer D. [^{125}I]Tyr^{10}-cortistatin$_{14}$ labels all five somatostatin receptors. *Naunyn-Schmiedeberg's Arch Pharmacol* 1998; 357:483–489.
25. Thoss VS, Pérez J, Probst A, Hoyer D. Expression of five somatostatin receptor mRNAs in the human brain and pituitary. *Naunyn-Schmiedeberg's Arch Pharmacol* 1996; 354:411–419.
26. Reubi JC, Kvols LK, Waser B, Nagorney D, Heitz PU, Charboneau JW, Reading CC, Moertel C. Detection of somatostatin receptors in surgical and percutaneous needle biopsy samples of carcinoids and islet cell carcinomas. *Cancer Res* 1990; 50:5969–5977.
27. Reubi JC. In vitro identification of vasoactive intestinal peptide receptors in human tumors: implications for tumor imaging. *J Nucl Med* 1995; 36:1846–1853.

28. Stolz B, Smith-Jones PM, Albert R, Reist H, Mäcke H, Bruns C. Biological characterisation of [^{67}Ga] or [^{68}Ga] labelled DFO-octreotide (SDZ 216–927) for PET studies of somatostatin receptor positive tumors. *Horm Metab Res* 1994; 26: 453–459.
29. Buscail L, Saint-Laurent N, Chastre E, Vaillant JC, Gespach C, Capella G, Kalthoff H, Lluis F, Vaysse N, Susini C. Loss of sst2 receptor gene expression in human pancreatic and colorectal cancer. *Cancer Res* 1996; 56:1823–1827.
30. Laws S, Gough AC, Evans AA, Bains MA, Primerose JN. Somatostatin receptors subtype mRNA expression in human colorectal cancer and normal colic mucosa. *Br J Cancer* 1997; 75:360–366.
31. Greenman Y, Melmed S. Expression of three somatostatin receptor subtypes in pituitary adenomas: evidence for preferential SSTR5 expression in the mammosomatotroph lineage. *J Clin Endocrinol Metab* 1994; 79:724–729.
32. Sharma K, Patel YC, Srikant CB. Subtype-selective induction of wild-type p53 and apoptosis, but not cell cycle arrest, by human somatostatin receptor 3. *Mol Endocrinol* 1996; 10: 1688–1696.
33. Sharma K, Srikant CB. Induction of wild-type p53, Bax, and acidic endonuclease during somatostatin-signaled apoptosis in MCF-7 human breast cancer cells. *Int J Cancer* 1998; 76: 259–266.
34. Virgolini I, Pangerl T, Bischof C, Smith-Jones P, Peck-Radosavljevic M. Somatostatin receptor subtype expression in human tissues: a prediction for diagnosis and treatment of cancer? *Eur J Clin Invest* 1997; 27:645–647.